ACADÉMIE
DES SCIENCES
INSTITUT DE FRANCE

Comptes Rendus
Physique

Ourouk Jawad, Emmanuelle Conil, Jean-Benoît Agnani, Shanshan Wang and Joe Wiart

Monitoring of the exposure to electromagnetic fields with autonomous probes installed outdoors in France

Published online: 15 May 2024

Part of Special Issue: Energy in the heart of EM waves: modelling, measurements and management

Guest editors: Emmanuelle Conil (ANFR, France), François Costa (ENS Paris-Saclay, Université Paris-Saclay, Université Paris-Est Créteil, France) and Lionel Pichon (CNRS, CentraleSupélec, Université Paris-Saclay, Sorbonne Université, France)

https://doi.org/10.5802/crphys.182

The Comptes Rendus. Physique *are a member of the Mersenne Center for open scientific publishing*
www.centre-mersenne.org — e-ISSN : 1878-1535

ACADÉMIE DES SCIENCES
INSTITUT DE FRANCE

Comptes Rendus. Physique
Published online: 15 May 2024
https://doi.org/10.5802/crphys.182

Research article / *Article de recherche*

Energy in the heart of EM waves: modelling, measurements and management / *L'énergie au cœur des ondes électromagnétiques : modélisation, mesures et gestion*

Monitoring of the exposure to electromagnetic fields with autonomous probes installed outdoors in France

Surveillance de l'exposition aux ondes électromagnétiques à l'aide de sondes autonomes installées en extérieur en France

Ourouk Jawad [*,a], Emmanuelle Conil [a], Jean-Benoît Agnani [a], Shanshan Wang [b] and Joe Wiart [c]

[a] ANFR, 78 avenue du général de Gaulle, 94700 Maisons-Alfort, France

[b] ETIS, UMR 8051, CY Cergy Paris Université, ENSEA, CNRS, F-95000, France

[c] Chaire C2M, LTCI, Télécom Paris, Institut Polytechnique de Paris, 91120 Palaiseau, France

E-mails: ourouk.jawad@anfr.fr (O. Jawad), emmanuelle.conil@anfr.fr (E. Conil), jean-benoit.agnani@anfr.fr (J.-B. Agnani), shanshan.wang@ensea.fr (S. Wang), joe.wiart@telecom-paris.fr (J. Wiart)

Abstract. The study is based on a new temporal analysis of exposure based on the deployment of autonomous broadband E-field monitoring probes in many French cities. The combination of the probe's data with frequency-selective in situ measurements performed by ANFR and the knowledge of the nearby base station antennas, allows to draw statistical conclusions on the exposure of the population. Indeed, the data collected by the probes reveal that different periodicities exist (seasonality, day/night). This paper shows that the monitoring probes are able to detect the seasonality of the exposure and provide analysis of correlation between monitoring probes and radio environment.

Résumé. L'étude repose sur une nouvelle analyse temporelle de l'exposition se basant sur le déploiement de sondes autonomes large bande pour la surveillance du champ électrique dans plusieurs villes françaises. La combinaison des données issues des sondes avec les mesures in situ sélectives en fréquences effectuées par l'ANFR et la connaissance des stations de base avoisinantes permet de tirer des conclusions sur l'exposition de la population. En effet, les données collectées des sondes révèlent que différentes périodicités existent (saisonnalité, jour/nuit). Cet article montre que les sondes sont capables de détecter la saisonnalité de l'exposition et de fournir une analyse de la corrélation entre les sondes et l'environnement radio.

* Corresponding author.

Keywords. Monitoring, Exposure, EMF, In situ measurement, Principal component analysis.

Mots-clés. Surveillance, Exposition, Champs EM, Mesure in situ, Analyse en composante principale.

Note. This article follows the URSI-France workshop held on 21 and 22 March 2023 at Paris-Saclay.

Funding. European Union's Horizon Europe Framework Programme under Grant Agreement number 101057622 (SEAWave Project).

Manuscript received 27 July 2023, revised 11 December 2023 and 5 March 2024, accepted 14 March 2024.

1. Introduction

The topic of assessing human exposure to electromagnetic waves is a continuous subject of discussion leading to important debates in society. Many studies have been conducted worldwide to assess the downlink human exposure due to mobile phone base stations or the uplink exposure due to personal equipment such as mobile phones [1, 2]. In France, the Agence nationale des fréquences (ANFR) is responsible for the surveillance of the exposure of the public to EMF. Thousands of in situ measurements are carried out every year [3], and ANFR has fine-tuned the level of exposure due to the deployment of 5G NR technology through measurements and simulations [4]. Furthermore, the compact electronic integration enables the development of new techniques for EMF monitoring. In fact, city councils and ANFR have installed tens of autonomous monitoring probes that perform broadband measurements of the electric field (E-field) several times a day [5]. This new measurement technique offers the possibility to analyze spatiotemporal variations of the exposure level in different radio environments.

The domain of the continuous monitoring of E-field has achieved several significant milestones. In [6–12], different networks of probes monitoring the E-field are presented. They are located in different countries: Belgium, Greece, Italy, Serbia and Spain. In most of the studies, probes are positioned at a fix position but in [6] they are not fixed. Many of the papers focus on the architecture of the probe networks such as [6, 9, 11] and do not go deeper in the statistical temporal analysis. In [7, 8, 10, 12], temporal analysis of the exposure reveals some interesting phenomena such as traffic fluctuation, variation between day and night or variation between urban and rural area. In [13], a systematic literature review was conducted on EMF exposure monitoring in various countries, the conclusion suggests that there is a need for a common method of temporal analysis. In [12], an important milestone is presented regarding the comparison of temporal analysis of the exposure to EMF in different European countries (Greece, Spain, Romania and Serbia). The study compares statistical parameters of the E-field on a yearly basis in different countries, but it does not include France.

For the first time, this paper presents an analysis of the time variation of the E-field in France by combining measurements by autonomous probe with other sources of information, including the database of in situ measurements and the database of base station antennas. For this purpose, the available data are presented: the database of in situ measurements, carried out near autonomous probes, the database of base station antennas and the database of monitoring probes. Afterwards, the methodologies are presented: a classical statistical analysis and principal component analysis (PCA) principles.

Then, the data analysis is carried out, beginning with a general statistical analysis that reveals daily fluctuations. A general analysis based on PCA is performed to know if there is any correlation between the evolution of the exposure level and the radio environment thanks to in situ measurements and the nearby base stations. The PCA is also used to detect the temporal patterns over 2022 and the spatial dependence on the radio environment. The results indicate that the techniques of statistical analysis are promising methods to reveal global and local patterns of the exposure related to the cellular network environment.

This article presents significant findings on the monitoring of the E-field. The day-and-night fluctuation of the level of exposure is analyzed, and an empirical day/night hour interval is found. Based on the monitoring probes data, for the first time, the daily variation is characterized and confirms the communicated uncertainty contributor. PCA method is used on two different datasets. First, PCA helps to identify the probes which are ideally positioned for monitoring of the exposure due to radio environment, and second, PCA demonstrates the presence of seasonality throughout the year.

2. Available data

2.1. *ANFR's base station antennas database*

ANFR provides open source data regarding exposure of the French population. There are two types of data available in raw data format or plotted on a map [3]. ANFR gives its legal agreement for the installation of base stations and keeps the French national antenna database up-to-date (for antennas with EIRP > 5 W). On the Cartoradio website, it is possible to check the installed base station antennas everywhere in France, including details such as technology (2G–5G), frequency band, mobile operator, azimuthal direction, height of the antenna [3]. Information is provided for different types of networks: TV broadcasting, radio broadcasting, point-to-point fixed radio relay and cellular network. In this article, only base station antennas are used. The Cartoradio website provides the locations of the base stations and shows locations where accredited in situ measurements have been carried out. Details of measurements and base stations are available by clicking on the indicators.

2.2. *Monitoring probe database*

City councils, ANFR, and the C2M team of Telecom Paris have installed autonomous monitoring probes. The monitoring probes were designed by the EXEM company and measure the three components of the E-field between 80 MHz and 6 GHz [14]. The autonomous probe measures the E-field level (equals to the square root of the sum of the squared components of the E-field) integrated over the whole frequency band [15]. Since 2019, 152 autonomous probes have been installed in different cities in France. In general, the probes are attached to outdoor electric poles or other street furniture at a certain height to avoid access by pedestrians (Figure 1). The probes measure at several times of the day and night: every two hours between 1:00 AM and 11:00 PM and each measurement is averaged over 6 min. A website provided by EXEM gives access to the measurement results of the probes [5]. Some of the autonomous probe monitoring data are made publicly available by city councils.

Table 1 below shows the number of autonomous probes per city, the name of the city or conurbation authority where probes are installed, and the department code. Cities and conurbation authorities identify interesting probe locations by targeting locations with a high density of base stations or near children's schools or major public places located in city centers.

2.3. *Broadband and frequency-selective in situ measurement database*

ANFR and its partners conduct thousands of in situ measurements annually. Any French resident can request an in situ measurement at home or in any public space. The accessible results include the broadband E-field measurement and the frequency-selective E-field measurement. In situ measurements follow the ANFR protocol [16], which is in line with standard EN IEC 62232:2022 [17]. The ANFR protocol provides a methodology to assess the level of exposure

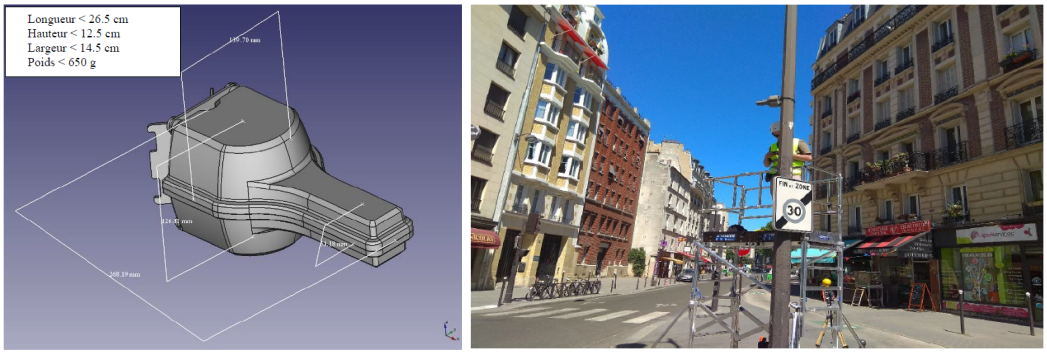

Figure 1. 3D shape of an autonomous probe and a picture taken during the installation of a probe on a street pole in Paris, extracted from EXEM datasheet [14].

Table 1. Number of probes per city or conurbation authority

Number of probes	Name of city or conurbation authority	Department name (number)
5	Lille Métropole	Nord (59)
9	Paris	Paris (75)
19	Massy	Essonne (91)
4	Grand Paris Sud	Essonne (91) and Seine-et-Marne (77)
7	Orléans Métropole	Loiret (45)
8	Eurométropole de Strasbourg	Bas-Rhin (67)
3	Mulhouse	Haut-Rhin (68)
10	Rennes	Ille-et-Vilaine (35)
50	Nantes Métropole	Loire-Atlantique (44)
33	Bordeaux Métropole	Gironde (31)
3	Marseille	Bouches-du-Rhône (13)

in France, while standard EN IEC 62232:2022 is the most detailed standard for determining RF field strength in the vicinity of the radiocommunication base stations. The ANFR measurement protocol is divided into two parts. The first part, called “case A”, consists of a broadband E-field measurement at three different heights (1.10 m, 1.50 m, 1.70 m); the level of exposure, expressed in V/m, is the root mean square (RMS) of the E-field measured at the three heights for six minutes. Usually, the position of the probe position is typically based on a hot-spot search, and the technician makes a few measurements to determine where the exposure is maximum. For the measurement at the ground level beneath the monitoring probe, the hot spot search is skipped. The second part of the measurement called “case B” consists of a frequency-selective E-field measurement at the same position as in case A. The results of the measurement provide an overview of the contributions of the different technologies using any bands between 100 kHz and 6 GHz.

ANFR regularly analyzes, the exposure to EMF due to base station antennas with:

- the yearly report which investigates the evolution of the exposure based on the outdoor and indoor in situ measurements (the yearly report is based on the measurement requested by French citizens) [18];
- the report investigating the evolution of exposure specifically due to the 5G deployment [19];

Table 2. Description of the ANFR databases

	Type of data	Description	Applicant
Base station antennas	Information	Base station antennas installed everywhere in France with description of technology (2G–5G), frequency band, mobile operator, azimuthal direction, height of the antenna	Mainly network operators request installation of base station antennas
Monitoring probes	Measurement	Monitoring probes measuring the three components of the E-field between 80 MHz and 6 GHz at multiple times of the day and night: every two hours between 1:00 AM and 11:00 PM and each measurement is averaged over 6 min	City councils, C2M team and ANFR are the main applicants for probe installation
In situ measurements	Measurement	Measurements in two parts: • Case A: broadband measurement at three heights for 6 min • Case B: frequency-selective measurement at the same position as case A from 100 kHz to 6 GHz	Usually, the applicants are citizens who ask for in situ measurements. In this study, ANFR asked for in situ measurements at the ground level under each probe

- the "city hall square" campaign, which is carried out every three years in more than 1000 cities (80% urban areas and sub-urban areas 20%) [20];
- and other specific campaigns (smart meters, subway etc.).

These reports show that in a very high majority of cases, the largest contribution to the overall exposure level is due to cellphone networks (59% in 2021). In more than 20% of the in situ measurements in 2021, there are no major contributions because the measured level is low and close to the sensitivity threshold of measurement instruments. For the rest of the in situ measurements, the major contributions can come from WLAN, HF bands, or private mobile radio.

2.4. *ANFR database in a glance*

In a nutshell, three databases from ANFR are used in this article. For the sake of clarity, these databases are presented at a glance in Table 2.

3. Methodology

3.1. *Classical statistical analysis*

The large amount of data enables to make classical statistical observations on the different magnitudes of the E-field measured by the probes. Since the measurements are made several times per day and per night, starting from the installation of the probe, it is possible to see if there is any common temporal behavior. Comparisons can be made between day and night exposure

levels, or between working hours and off-duty hours. Since the E-field is measured by the probe in volts per meter, the root mean square is used to evaluate the mean of the E-field. For a more general analysis of the variation during 2022, a more sophisticated statistical method must to be used, in particular to correlate the level of exposure with the radio environment. Indeed, the first section highlighted that the seasonality of France has never been shown, and that the correlation with radio environment data has never been done either.

3.2. *Principal component analysis (PCA)*

PCA is a popular method for analyzing high-dimensional data [21]. It is an unsupervised statistical method that allows large datasets of correlated variables to be reduced to a smaller number of uncorrelated principal components that explain most of the variability in the original dataset. Suppose that the dataset X is an N-by-P matrix, where N observations are the rows of the X matrix and P variables are the columns of the X matrix. There are mainly four steps involved in PCA:

(1) Centralization of the dataset X to characterize deviations between the observations. It consists in subtracting the mean value of each variable (i.e. column of X).
(2) Computation of the covariance matrix.
(3) Computation of eigenvalues and eigenvectors of the covariance matrix to identify the principal components. Our principal components that maximize the variance of all projected points onto a 2D space is the eigenvector of the covariance matrix associated with the largest eigenvalue. There are several techniques to compute eigenvalues and eigenvectors, one of the most used within PCA and in this study is the Singular Value Decomposition.
(4) Extraction of scores and loadings: the PCA is then based on the decomposition of the data matrix into two matrices V and U. The matrix V is a k-by-P (where k is the number of principal components) matrix and is usually called the loading matrix. The loadings can be understood as the weights for each original variable in the principal components space. The matrix U is called the score matrix. It contains the original observations in a rotated coordinate system.

PCA is a well-known method to reduce the dimensions of a data set. In our case, it may be helpful to find the main components that characterize the time variability between the autonomous probe measurements. PCA would help to determine whether the recorded shapes of the monitoring probe level have similarities or differences.

4. Data analysis

4.1. *Autonomous probe variability analysis*

In this section, data from monitoring probes described in Section 2.2 are used. Figure 2 displays the Cumulative Distribution Function (CDF) of 110 monitoring probes. The CDF plotted on Figure 2 gather measurements during the year 2022. The average value of the numbers of measurements used to build CDF is 4325 measurements per probe. This figure shows the extend of measured values by monitoring probes. It shows that for a large number of monitoring probes, the measured values are below 1 V/m. These plots also show that the number of measurements is very high and that advanced techniques must be used in order to handle the variability between probes.

Raw data of the E-field measured by probes are too difficult to analyze (raw data of all monitoring probes are presented in Figure 3 without filtering for the year 2022), then a selection

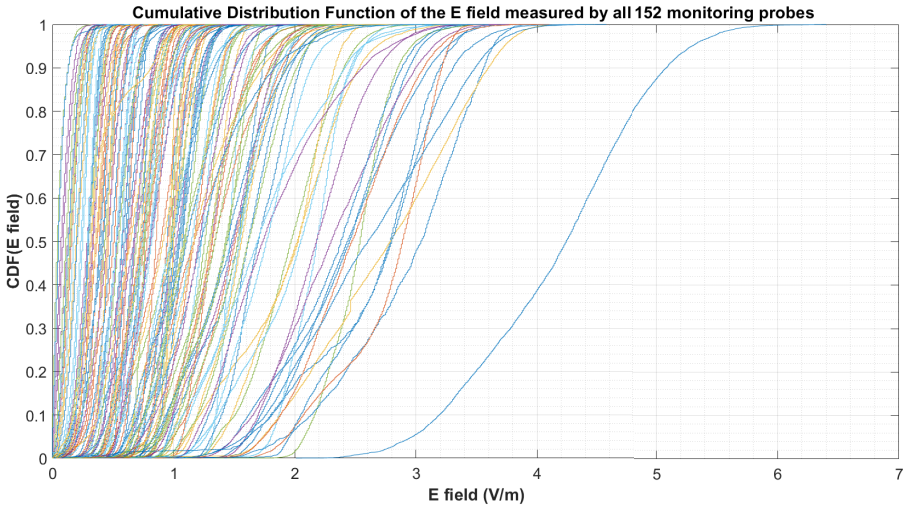

Figure 2. Cumulative Distribution Functions of E-field measured by probes which were operating during 2022.

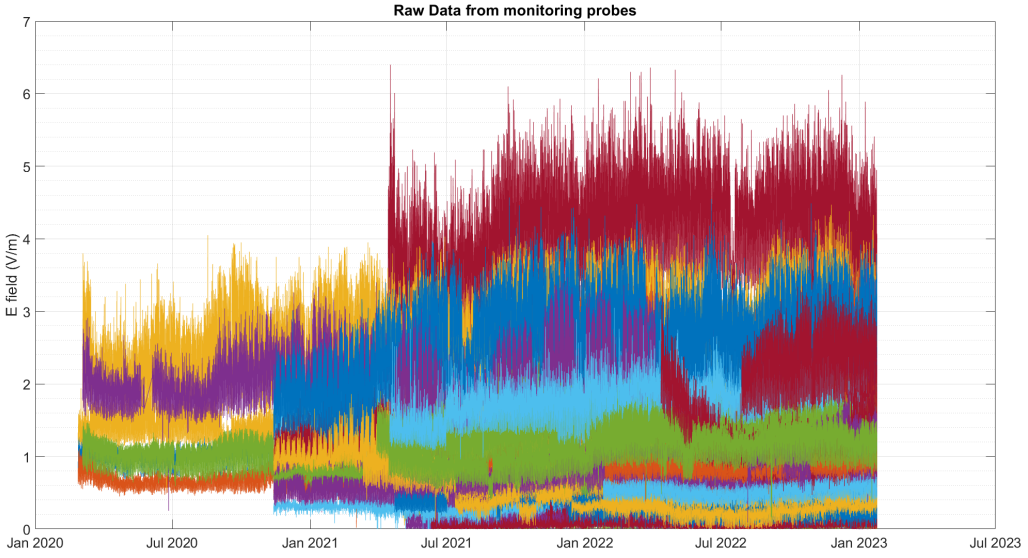

Figure 3. Raw data of E-field measured by all the probes since installation, showing fast variation on a daily basis and very low variation over long periods of time.

of a few probes is necessary. As a starting point, the RMS of the E-field of each probe was calculated, and we selected three probes with the highest RMS value. The RMS value was calculated over the data measured during the year 2022.

A deeper analysis can be made, based on a different time scale analysis. Indeed, since measurements are made day and night, a remaining question is how the level of exposure is evolving between day and night. Figure 4 shows CDF of the 3 selected probes (highest RMS) with an empirical time separation: day is between 8 AM and 11 PM and night is between 11 PM and 8 AM. This plot shows that for the three highest probes the differences are remarkable. In fact, the

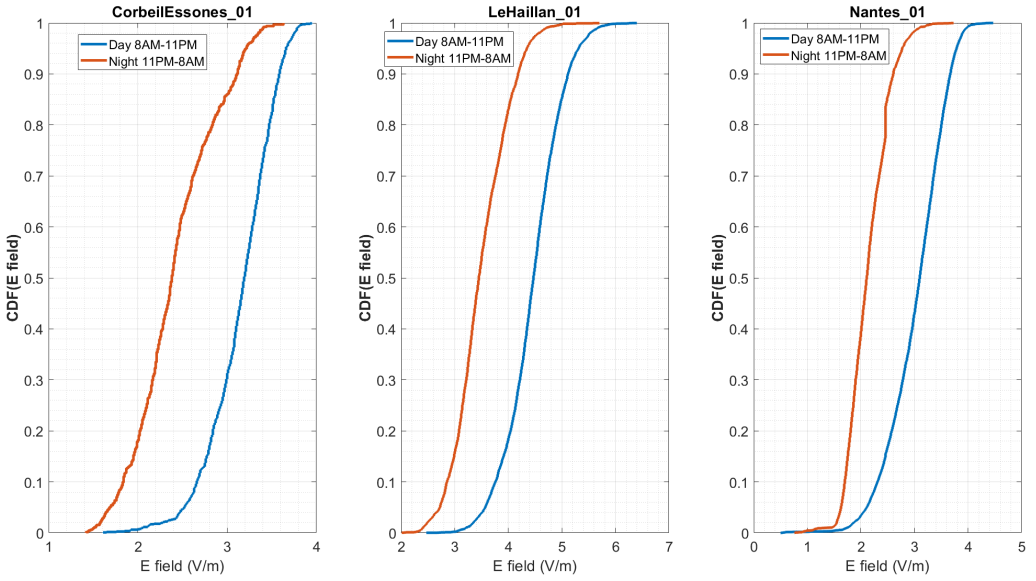

Figure 4. Day and Night CDF of selected probes (Day 8 AM–11 PM and Night 11 PM–8 AM).

ratio of the average day-value over the average night value is 1.30 for CorbeilEssones_01, 1.28 for Le Haillan_01, 1.42 for Nantes_01. For the probes with the lowest RMS level (not presented in this article), the level of exposure is not different during the night compared to the day. This is due to the fact that the lowest RMS probes are installed far from base station antennas and therefore measure very low levels.

The number of measurements and the coverage of many different cities (urban and suburban) allow for another type of analysis. Figure 5 displays the coefficient of variation (also called relative standard deviation) calculated on the basis of the measurements made during working days and hours (Monday to Friday from 8 AM to 5 PM). Figure 5 shows that the coefficient of variation is less than 30% for 86% of the probes. For the 21 probes with variation coefficients higher than 30%, most of the probes measure very low levels of exposure or have large variations due to repairs. This information is valuable for ANFR because the uncertainty budget of the accredited in situ measurements includes a specific contributor for the daily time variation which is equal to 30%. It confirms that the uncertainty contributor due to daily variation is up to 30% and it is consistent with the information provided by ANFR.

4.2. *Data preparation prior to PCA*

4.2.1. *Dataset No. 1*

The purpose of this study is to correlate E-field measurements from monitoring probes with the radio environment. The radio environment is described by two sources of data. The first source of data consists of the “case B” measurement, also known as the frequency-selective E-field measurement per band. The bands covered are 700 MHz, 800 MHz, 900 MHz, 1800 MHz, 2100 MHz, 2600 MHz and 3600 MHz and they encompass every technology (GSM/GPRS, UMTS, LTE and 5G EN-DC) available in France. The second source of data is the number of base station antennas near the probe’s location. The idea is to tally the number of base station antennas per band that fall within a circle surrounding each probe. Figure 6 is a schema illustrating how

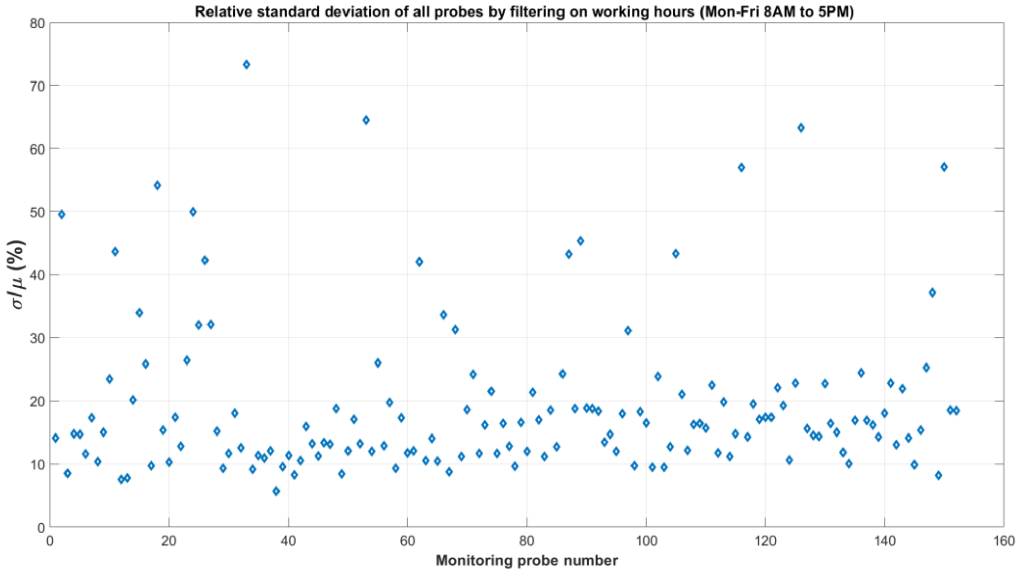

Figure 5. Relative standard deviation of all probes by filtering on working hours (Monday to Friday from 8 AM to 5 PM).

base station antennas are included in the final count. The antennas are oriented to radiate towards a specific direction (called azimuthal direction of radiation, called α and α' in Figure 6) to cover a specific cell. Within the circle surrounding the probe, certain base station antennas are mechanically oriented towards the probe, while others are not. A base station antenna is considered if the bearing angle β (respectively β') of the vector going from the antenna to the probe is in the interval $[\alpha - \Delta\phi/2,\ \alpha + \Delta\phi/2]$ (respectively $[\alpha' - \Delta\phi/2,\ \alpha' + \Delta\phi/2]$). A standard 120° angular spread ($=\Delta\phi$) is used. This rule applied to the base station antennas in Figure 6 means that only one base station is considered in the final count. Regarding the radius of the circle, the assumption has been made that antennas oriented towards the probe and located at a distance of less than 400 m should be counted for each cellular band. The rationale behind this assumption is that for a typical antenna EIRP (average EIRP is 32.6 dBm based on the ANFR base station antenna database) and a distance of 400 m, the E-field in free space can be estimated to be less than 0.02 V/m, which appears to be sufficient to include any contributor per band.

For the sake of clarity, Figure 7 represents the matrix X for dataset No. 1, composed of variables coming from the three databases:

- squared of the E-field monthly averaged from monitoring probe database;
- squared of the E-field per band from case B in situ measurement database;
- and, the number of base stations per band surrounding monitoring probes from the base station antenna database.

In order to make sure that the measurements of monitoring probes are comparable to in situ measurements, a comparison has been made. The Figure 8 presents the comparison of RMS of E-field measured by probes with in situ case A measurements. It appears that the plot is almost linear, which means that both techniques of measurement provide close results. In situ measurement (carried out by ISO17025 accredited laboratories) uncertainty budget ($k = 1.96$) for case A is 2.3 dB and the monitoring probe estimated uncertainty of measurement is 3.8 dB in case the entire bandwidth is considered [3]. The combined uncertainty is equal to 4.1 dB, based on metrology rules, 95% of relative deviation between in situ measurements and E-field measured

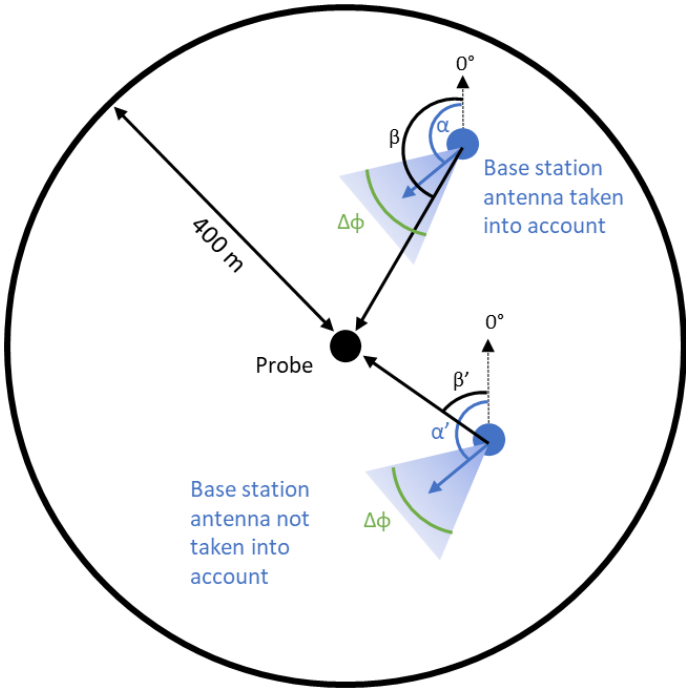

Figure 6. Schema explaining how base station antennas are considered in the final count.

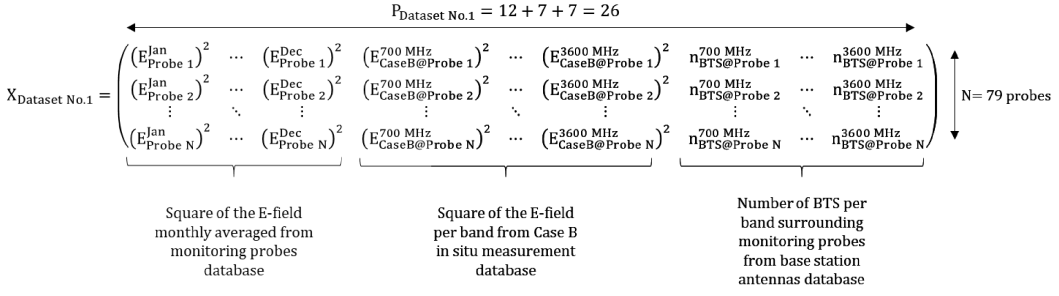

Figure 7. Input matrix for PCA on Dataset No. 1 with indication of the original database.

by the monitoring probes should be within the combined uncertainty. The relative deviations between both techniques of measurement reveal that 95.3% of relative deviations are within the combined uncertainty. This result means that monitoring probes and in situ measurement results are close, even if the measurement positions are separated by a few meters.

As explained in Section 3.1, the dataset needs to be standardized, so in our case it is preferable to use the square of the E-field. The dataset No. 1 is then composed of the following variables: the square of the E-field averaged for each month from January to December 2022, the square of the case B in situ E-field measured under the probes for each band, and the number of base station antennas within the 400 m radius for each band. To facilitate the interpretation of the PCA, the monitoring probes that measure relatively low levels of exposure have been filtered out. The threshold was chosen based on the average outdoor level of exposure measured by ANFR, based on thousands of measurements carried out over many years, and the probes with a 99th

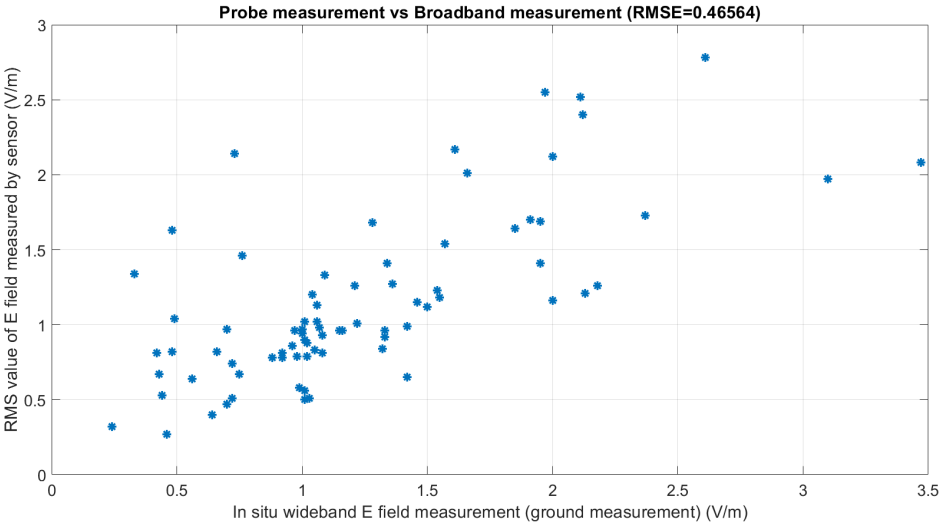

Figure 8. RMS value of E-field measured by monitoring probe (on the same day) in function of in situ broadband E-field measurement ("case A") at the ground under the probe.

$$\mathrm{P_{Dataset\ No.2}} = 12$$

$$\mathrm{X_{Dataset\ No.2}} = \begin{pmatrix} \left(\mathrm{E^{Jan}_{Probe\ 1}}\right)^2 & \cdots & \left(\mathrm{E^{Dec}_{Probe\ 1}}\right)^2 \\ \left(\mathrm{E^{Jan}_{Probe\ 2}}\right)^2 & \cdots & \left(\mathrm{E^{Dec}_{Probe\ 2}}\right)^2 \\ \vdots & \ddots & \vdots \\ \left(\mathrm{E^{Jan}_{Probe\ N}}\right)^2 & \cdots & \left(\mathrm{E^{Dec}_{Probe\ N}}\right)^2 \end{pmatrix} \quad \mathrm{N = 79\ probes}$$

Figure 9. Input matrix for PCA on Dataset No. 2.

percentile below 1 V/m were filtered out. The input matrix is composed of $P = 26$ variables and $N = 79$ observation probes.

4.2.2. *Dataset No. 2*

Dataset No. 2 focuses solely on the time domain, i.e. the square of the E-field measured by the monitoring probes from January to December 2022. The objective is to detect any time patterns along the monitoring probes, using the same exposure level filter as in dataset No. 1. The input matrix consists of $P = 12$ variables and $N = 79$ observation probes. For the sake of clarity, Figure 9 represents the matrix X for dataset No. 2, composed of variables coming from the monitoring probes database.

4.3. *PCA's results*

4.3.1. *Dataset No. 1*

Figure 10 shows the dataset No. 1 represented in the two main principal component coordinates. The probes are represented with different markers for each French department. Table 3

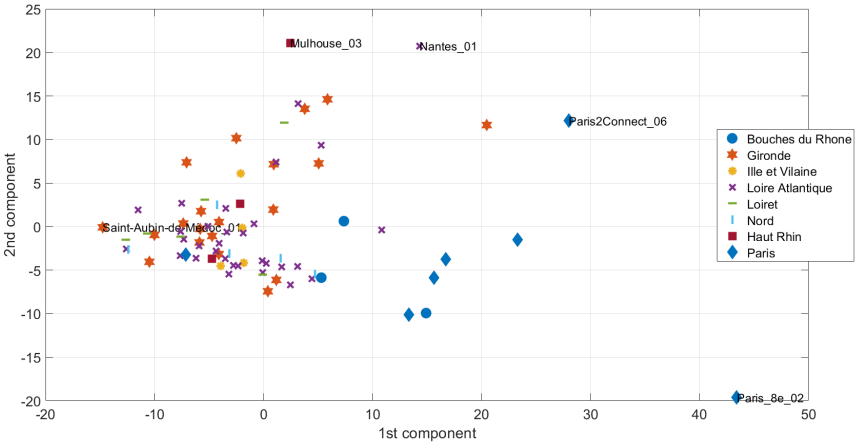

Figure 10. Dataset No. 1 represented on the domain composed by two main principal components.

Table 3. Eigen values for each component and proportion of explained variance for dataset No. 1

# Components	Eigenvalue	Proportion of total explained variance (%)
1	92.3991	62.3
2	46.8840	31.6
3	3.1131	2.1
4	1.5063	1.0
5	1.0244	0.7
6	0.8020	0.5

presents the eigenvalues and the percentage of total explained variance providing insight into the importance of the components in terms of variability. The choice has been made to display only six first parameters in the table. The proportion of total explained variance shows that the first two components represent 94% of the variability.

The point cloud represented in Figure 10 characterizes most of the variability of the original dataset. It means that distant points along the first or second components are very different from each other with respect to their original data. In Figure 10, some distant points/probes in the two principal component coordinate systems are selected. The name of distant probes selected are displayed on the plot. The selection of these probes (Saint-Aubin-de-Médoc_01, Mulhouse_03, Nantes_01, Paris2Connect_06, Paris_8e_02) for deeper analysis has the advantage of surrounding the point cloud and of giving a good interpretation on characterized variability.

Figure 11 shows the correlation circle for the original variables of dataset No. 1 represented in the domain of two components found by PCA. The “Months variable group” is the average monthly squared E-field by the probes, the “in situ frequency selective squared of the E-field variable group” comes from the result of case B measurement per band at the ground level and the “#Antennas variable group” are the number of base station antennas surrounding the probes. It shows that the number of base station antennas per band surrounding the probes is highly correlated with the first component, and that the level of exposure measured by probes and averaged monthly is highly correlated with the second component. The level of exposure

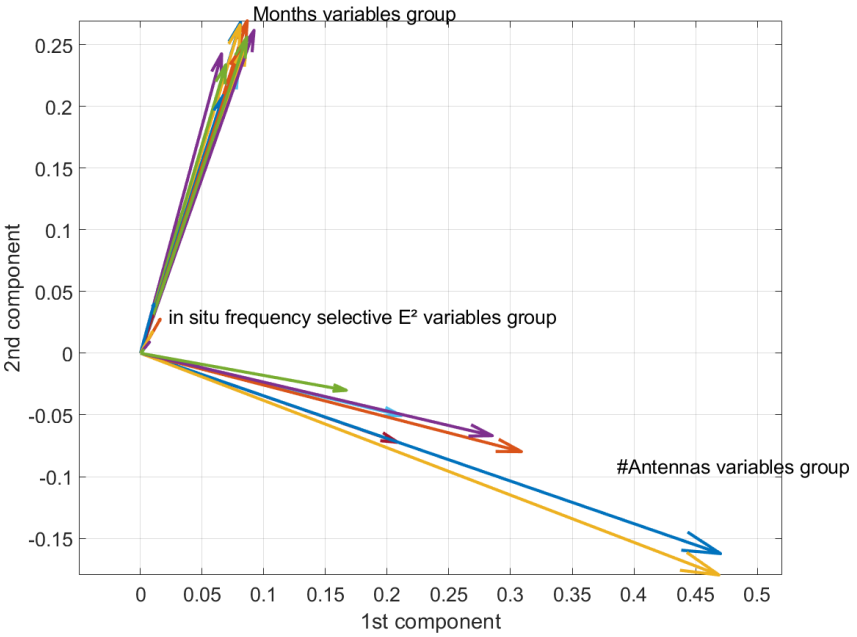

Figure 11. Correlation circle for dataset No. 1 representing variables projected on the two main components.

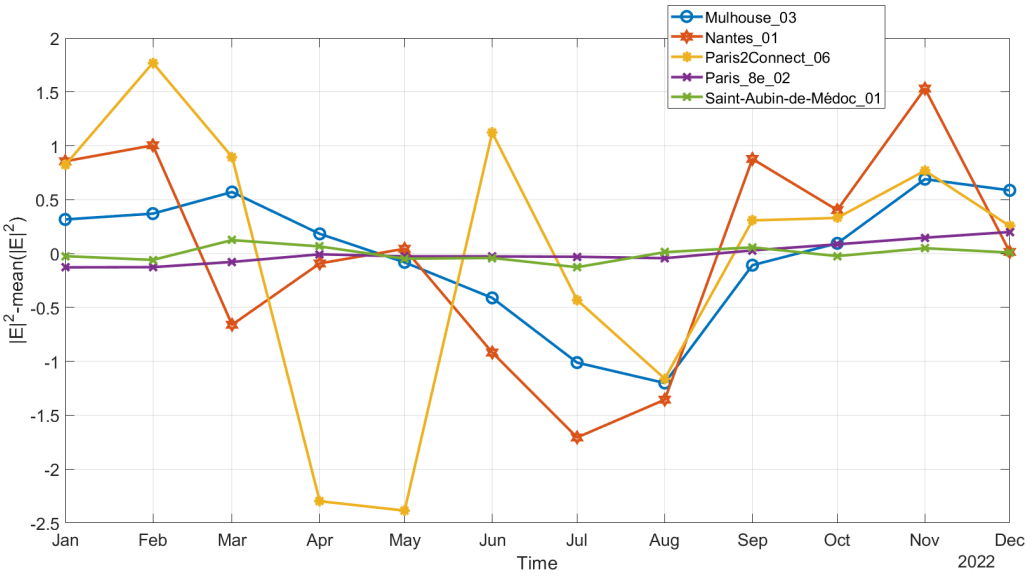

Figure 12. Square of the E-field during 2022 for the probes surrounding the principal components.

measured through case B measurements on the ground is more correlated with the second component than with the first.

To analyze the principal components characterization, the original data has been plotted for the five probes surrounding the point cloud. Figure 12 represents the square of the E-field per month minus its yearly average for the five probes surrounding the two components space.

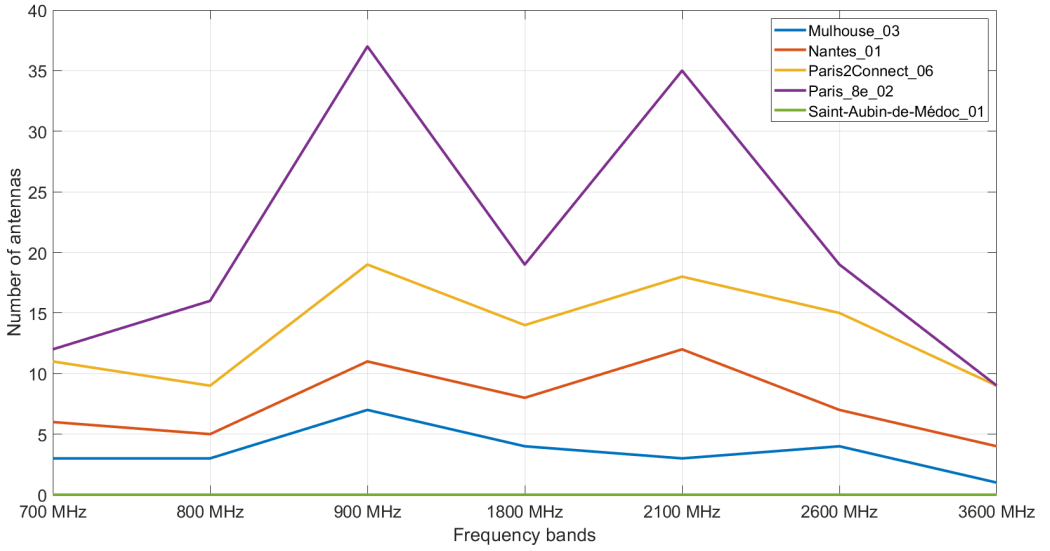

Figure 13. Number of base station antennas close to the probes surrounding the principal components.

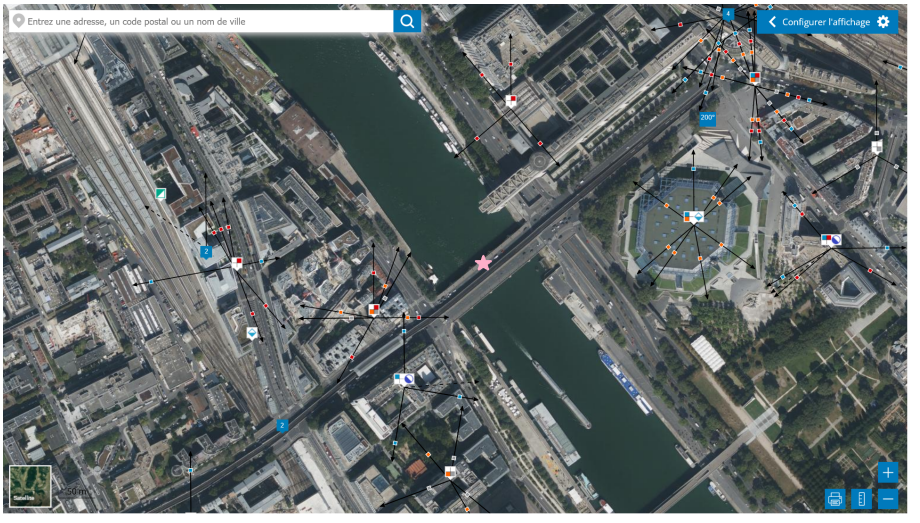

Figure 14. Picture of the position of the Paris2Connect_06 probe with surrounding base station antennas.

Figure 13 represents the number of base station antennas per band for the probes surrounding the two component space. The PCA reveals that the first component distinguishes between the probes located near a high number of base station antennas (on the right side) and those located near very few antennas (on the left side). The second component separates the probes with a high variability (top side) from those with very low variability (bottom side). These interpretations can be confirmed by comparing the locations of the different probes. Mulhouse_03, Nantes_01 and Paris2Connect_06 are installed in open areas (in front of a market, university hospital, or in the middle of a bridge) but with a high density of base station antennas. The Paris8e_02 probe

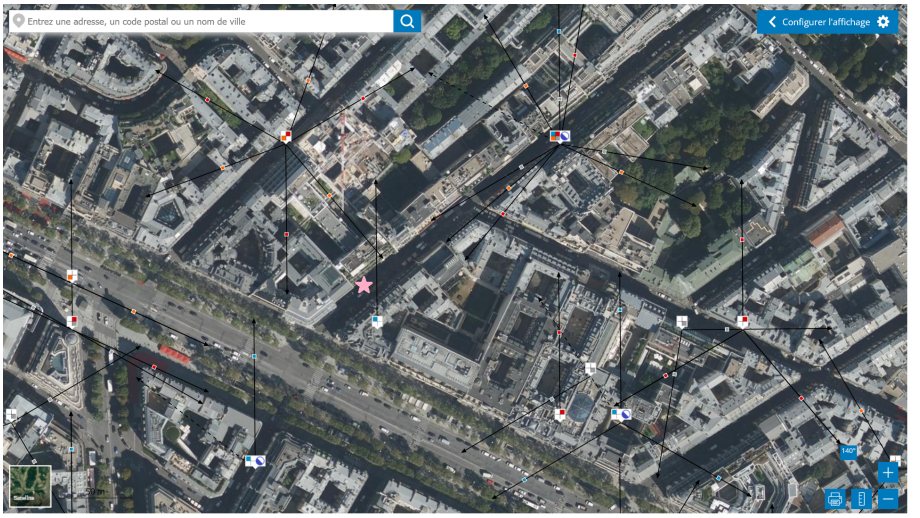

Figure 15. Picture of the location of the Paris8e_02 probe with surrounding base station antennas.

is located in a highly concentrated area of base station antennas near the Avenue des Champs Elysées, despite being situated on a narrow street without line-of-sight exposure. Figure 14 displays the location of the Paris2Connect_06 probe (pink star) with surrounding base station antennas, the arrows indicating the azimuthal directions of the base station antennas. Figure 15 displays the location of probe Paris8e_02 with surrounding base station antennas. Since the PCA shows that there is a correlation (Figure 11) between the continuous broadband monitoring of the E-field and the frequency-selective case B measurements, it is worth investigating the impact of base station antennas on exposure levels. Figure 16 presents the frequency-selective[1] measurements of the E-field for the surrounding probes of the PCA on dataset No. 1 (Mulhouse 03, Nantes_01, Paris2connect_06, Paris_8e_02 and SaintAubindeMedoc_01). It shows that the main contribution to the exposure level comes from cellular networks. Moreover, it shows that Mulhouse_03, Nantes_01 and Paris2Connect_06 have higher contributions in cellular bands than Paris_8e_02 and SaintAubindeMedoc_01. The cellular contributions of Paris_8e_02 and SaintAubindeMedoc_01 are close to the noise level of the measurement system. It confirms that the PCA on dataset No. 1 reveals:

- probes located in a dense area of base station antennas and measuring a high variability of exposure levels (high level on 1st component and high level on 2nd component, for instance Paris2Connect_06);
- probes located in a dense area of base station antennas and measuring a low variability of exposure levels (high level on 1st component and low level on 2nd component, for instance Paris_8e_02);

[1] Detailed frequency bands: HF = [100 kHz; 30 MHz], Private Mobile Radio (PMR) = [30 MHz; 47 MHz] ∪ [68 MHz; 87.5 MHz], FM Broadcasting = [87.5 MHz; 108 MHz] ∪ [174 MHz; 223 MHz], PMR/Radio Beacon = [108 MHz; 880 MHz] ∪ [921 MHz; 925 MHz], TV = [47 MHz; 68 MHz] ∪ [470 MHz; 694 MHz], 700 MHz band = [758 MHz; 788 MHz], 800 MHz band = [791 MHz; 821 MHz], 900 MHz band = [925 MHz; 960 MHz], Radars/Radio beacon = [960 MHz; 1710 MHz], 1800 MHz band = [1805 MHz; 1880 MHz], DECT = [1880 MHz; 1900 MHz], 2100 MHz band = [2100 MHz; 2170 MHz], 2600 MHz band = [2620 MHz; 2690 MHz], 3600 MHz band = [3490 MHz; 3800 MHz], Radars/Wireless local loop (WLL) = [2200 MHz; 6000 MHz], WLAN [2400 MHz; 2483.5 MHz] ∪ [5150 MHz; 5350 MHz] ∪ [5470 MHz; 5725 MHz].

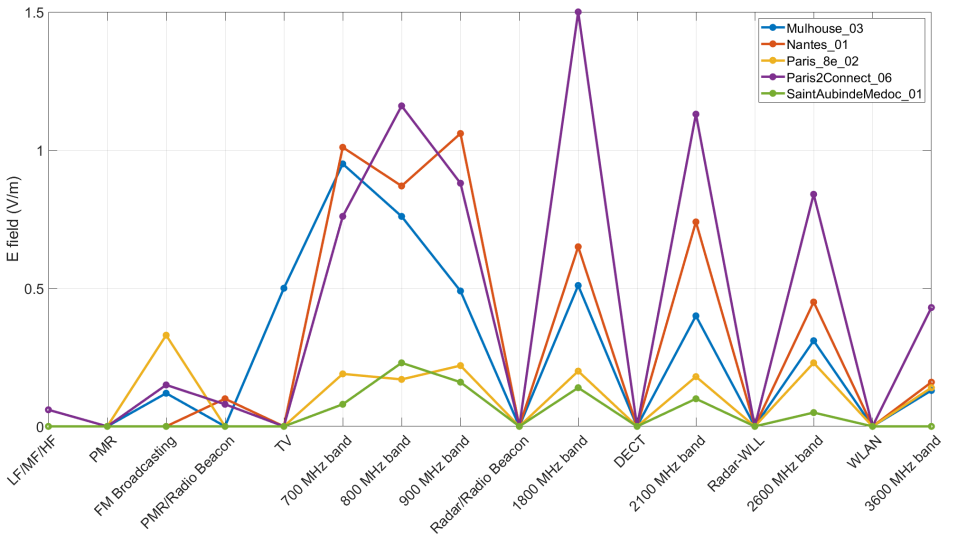

Figure 16. Frequency-selective E-field measurements (case B) for surrounding probes of PCA.

- probes located in a relatively dense area of base stations antennas and measuring a high variability of exposure levels (average level on 1st component and high level on 2nd component, for instance Mulhouse_03 and Nantes_01);
- probes located in the vicinity of few base station antennas and measuring a very low variability of exposure levels (low level on both components, for instance SaintAubindeMedoc_01).

4.3.2. *Dataset No. 2*

In Figure 17, Dataset No. 2 is represented in the two main principal component coordinates. Similar to dataset No. 1, the most distant probes surrounding the point cloud in the principal component graph are selected to highlight most of the variability. Table 4 presents the eigenvalues and the percentage of total explained variance, which gives an idea of how important the components are in terms of variability. The proportion of total explained variance shows that the first two components represent 98.5% of the variability. Figure 18 displays the correlation circle for the original variables of dataset No. 2 represented in the domain of two components found by PCA. It indicates that all months are equally correlated to the first component but the second component distinguishes summer months (top side) from winter months (bottom side). Figure 19 illustrates the original dataset No. 2 for the five probes surrounding the point cloud.

The PCA on dataset No. 2 shows that the first component distinguishes probes with high variability from those with low variability. The second principal component distinguishes probes installed in cities where the population density is higher in summer compared to winter, especially cities located in the south of France. Indeed, Orléans_01 is located near a skating rink and a school while Bègles_01 is located near a big hub of railway lines connecting to the Bordeaux-Saint-Jean train station. Marseille_03 is situated near the beach in downtown Marseille. It can be assumed that the probes surrounding the second component of the PCA in Figure 17 (Marseille_03, Bègles_01) experience a higher level of exposure during the summer months due to

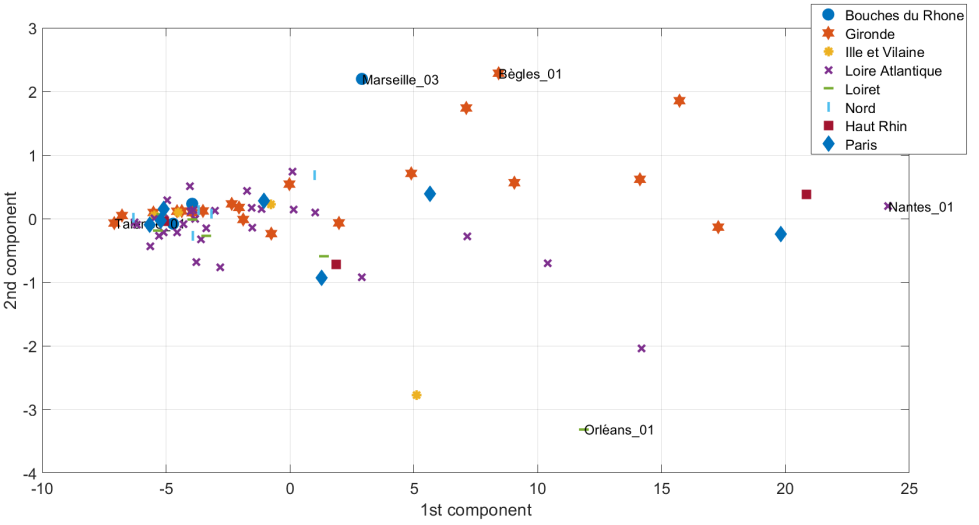

Figure 17. Dataset No. 2 represented on the domain composed by two main principal components.

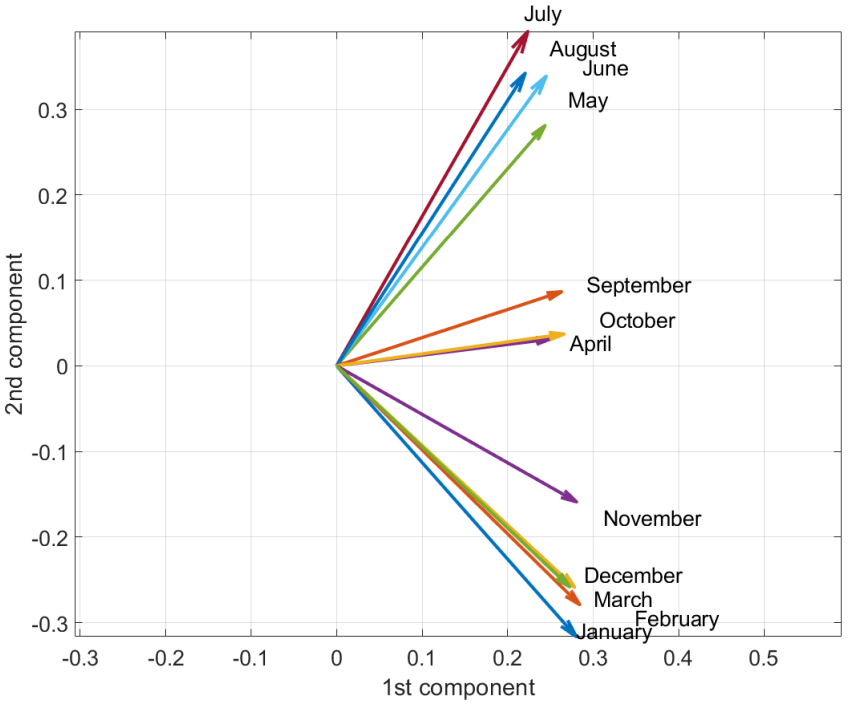

Figure 18. Correlation circle for dataset No. 2 representing variables projected on the two main components.

their proximity to frequently used areas (beach and railway lines) during summer time. The Orléans_01 probe measures low level of exposure during summer time because the skating rink and schools are closed during the summer months.

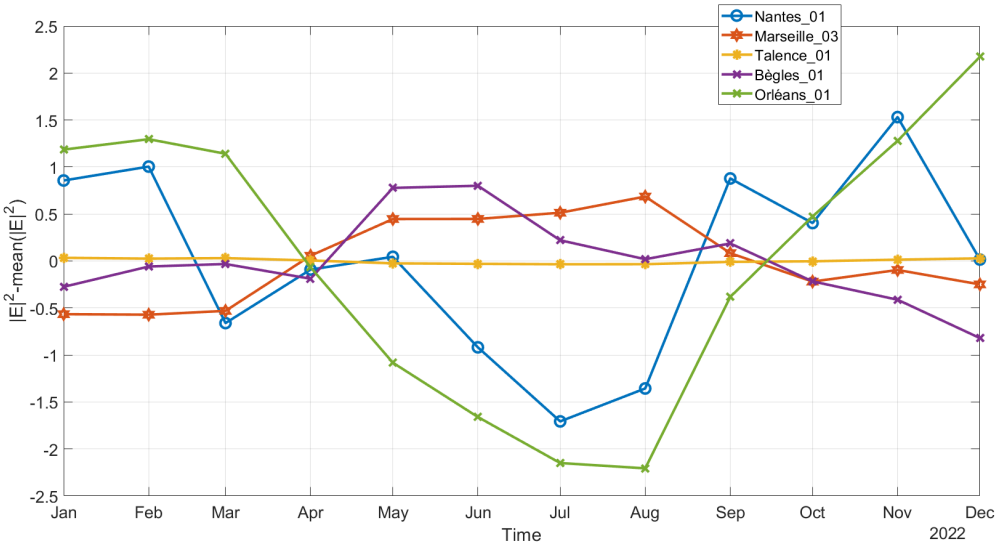

Figure 19. Square of the E-field during 2022 for the probes surrounding the principal components.

Table 4. Eigen values for each component and proportion of explained variance for dataset No. 2

# Components	Eigenvalue	Proportion of total explained variance (%)
1	50.6853	97.4
2	0.6201	1.1
3	0.2890	0.6
4	0.1992	0.4
5	0.0867	0.2
6	0.0605	0.1163

4.4. *Discussion of PCA results*

4.4.1. *Dataset No. 1*

Dataset No. 1 includes monthly averaged E-field measurements from monitoring probes, frequency-selective E-field measurements (case B) from in situ measurements and the number of base station antennas per cellular band surrounding each probe. The purpose of this dataset is to examine the correlation between the level measured by autonomous probes and the radio environment described by case B in situ measurements and number of base station antennas surrounding the probe. Principal component analysis has revealed probes that are located in dense areas of base station antennas or probes positioned in areas with very few base station antennas. PCA reveals probes that measure a high level of variability and are strongly dependent on the radio environment (high level on 1st component, high level on 2nd component). PCA reveals probes which measure a low level of variability and are not impacted by the radio environment (high level on 1st component, low level on 2nd component). Finally, the PCA of Dataset No. 1 reveals probes that are positioned correctly to monitor the E-field produced by the radio environment. Probes measuring a very low level of exposure can then be identified easily

and repositioned to positions that lead to a higher fluctuation of the exposure levels. However, some probes are positioned close to specific buildings (such as schools) and their role is to monitor low levels of exposure.

4.4.2. *Dataset No. 2*

Dataset No. 2 contains monthly averaged squared E-field measurements from monitoring probes. The purpose is to analyze whether there is a seasonal pattern within the monitoring probes. The principal component analysis on dataset No. 2 highlights probes that measure temporal E-fields that present a seasonal pattern. Indeed, probes with 1st component value higher than zero show a seasonal pattern, probes with high value on the 2nd component show a higher average level of exposure during summer time compared to winter time. Probes with negative level on the 2nd component present a higher averaged level of exposure during winter compared to summer. Finally, PCA helps us to identify the probes measuring seasonal patterns (1st component > 0), but also identifies how the summer season is compared to the winter. It shows that the type of neighborhood where the probe is installed plays a significant role.

5. Conclusion and perspectives

This study introduces a novel method for monitoring exposure to electromagnetic fields emitted by radio base stations. It shows that monitoring probes installed by ANFR, the C2M team of Télécom Paris, city councils or metropolitan authorities enable the analysis of the time domain aspect of exposure and the extraction of several noteworthy observations.

The analysis indicates that the monitoring probes have varying exposure levels. Probes measuring significant levels show a difference in exposure between day and night, a phenomenon observed for the first time in France. An empirical time interval from 8 AM to 11 PM enables to calculate the ratio of averaged E-field levels between day and night. This ratio is between 1.28 and 1.42 for the three probes with the highest RMS level. Several papers, such as [8–10], have characterized the day and night fluctuation, but this has never been demonstrated using French data.

For the first time, the variability of daily working hours has been quantified for all the probes installed in France. The data shows that most of the probes exhibit a 30% variation percentage based on the data gathered from 8 AM to 5 PM. Based on our knowledge, this is the first time that the assessment of the daily variation contributor based on more than 150 probes installed in different environments is achieved. It confirms the level of daily variation contributor to the in situ measurement uncertainty budget, as communicated in the accredited in situ measurement reports [3, 16, 17].

In this study, one of the goals was to correlate different sources of measurement: monitoring probe measurements and in situ measurements. In [12], an attempt was made to compare different types of monitoring probes installed in various countries. However, in this study, we compare in situ measurements to monitoring probes. It has been shown that measurements by monitoring probes installed on street furniture and in situ measurements on the ground level beneath the probes are nearly linear and that the relative deviations are bounded by the combined uncertainty. This is a satisfactory result, particularly given that the in situ measurement is taken only a few meters below the monitoring probe.

The published literature has shown several examples of monitoring probes [6–13], but for the first time a methodology based on PCA on dataset No. 1 has enabled the detection of probes that are in the best position to monitor radio environment radiation. Although the effect of antenna density on the measured field has been addressed in many studies mentionned in the introduction, for the first time, a methodology is proposed to detect which probes present a

strong correlation with antenna density. This methodology can also be useful to displace some of the probes which are installed in high density of base station area but not in a good configuration of exposure.

For the first time, the seasonality of the level of exposure has been analyzed at the French national level. The PCA on dataset No. 2 emphasizes the observation that the positioning of the probe is crucial to observe a remarkable variation of the exposure level. The probe must not only be installed in an area with many base stations, but also in close proximity to them and in a line-of-sight position for the exposure. A large number of probes measuring low exposure levels can be explained by the fact that the probes are not in a line-of-sight situation. In some cities, probes were installed in low-density areas rather than in front of base stations due to public concern over electromagnetic waves. Upon analysis, we find that some probes measure a lower level of exposure in summer time. This interpretation was confirmed with the Principal Component Analysis, which showed that the second component of the PCA characterizes the difference between probes with higher exposure in summer or winter. This phenomenon can be explained by the fact that some of the cities are very touristic during the summer, leading to increased use of the telecommunication infrastructure. In general, the exposure levels measured by the autonomous probe are very low compared to the limits. The increase of the exposure level is relatively slow, as it has been shown in several ANFR studies [4, 18–20].

In future work, statistical clustering methods can be used to group probes in PCA coordinates and enhance the methodology for detecting probes with the same E-field pattern.

Declaration of interests

The authors do not work for, advise, own shares in, or receive funds from any organization that could benefit from this article, and have declared no affiliations other than their research organizations.

Funding

Funding for this research was provided by the European Union's Horizon Europe Framework Programme under Grant Agreement number 101057622 (SEAWave Project) [22].

Acknowledgments

We thank C2M Telecom Paris for their very valuable input. We greatly acknowledge EXEM company (ANFR's subcontractor) for conducting in situ measurements, installing monitoring probes, and sharing all the probe results with ANFR.

References

[1] WHO, The International EMF project, https://www.who.int/initiatives/the-international-emf-project/.

[2] ICNIRP, "Guidelines for limiting exposure to electromagnetic fields (100 kHz to 300 GHz)", *Health Phys.* **118** (2020), no. 5, p. 483-524.

[3] Cartoradio by ANFR, "La carte des sites et des mesures radioélectriques", https://www.cartoradio.fr/.

[4] ANFR, "Multiple reports on exposure to 5G technology", https://www.anfr.fr/maitriser/les-installations-radioelectriques/etudes-sur-les-installations-radioelectriques/5g.

[5] Observatoire des ondes, https://www.observatoiredesondes.com/fr/.

[6] J. Wout, V. Leen, T. Emmeric, M. Luc, "In-situ measurement procedures for temporal RF electromagnetic field exposure of the general public", *Health Phys.* **96** (2009), no. 5, p. 529-542.

[7] D. Gallo, C. Landi, N. Pasquino, "Multisensor network for urban electromagnetic field monitoring", *IEEE Trans. Instrum. Meas.* **58** (2009), no. 9, p. 3315-3322.
[8] M. Athanasios, B. Achilles, S. Theodoros, J. N. Sahalos, "Continuous electromagnetic radiation monitoring in the environment: analysis of the results in Greece", *Radiat. Prot. Dosim.* **151** (2012), no. 3, p. 437-442.
[9] D. Nikola, K. Dragan, K.-L. Karolina, B. Vera, "The SEMONT continuous monitoring of daily EMF exposure in an open area environment", *Environ. Monitor. Assessment* **187** (2015), article no. 191.
[10] D. Luis, R. Agüero, L. Muñoz, "Electromagnetic field assessment as a smart city service: the smartsantander use-case", *Sensors* **17** (2017), no. 6, article no. 1250.
[11] N. Djuric, N. Kavecan, M. Mitic, N. Radosavljevic, A. Boric, "The concept review of the EMF RATEL monitoring system", in *2018 22nd International Microwave and Radar Conference (MIKON), Poznan, Poland*, 2018, p. 258-260.
[12] I. Serafeim, C. Apostolidis, A. Manassas, T. Samaras, "Electromagnetic fields exposure assessment in Europe utilizing publicly available data", *Sensors* **22** (2022), no. 21, article no. 8481.
[13] S. Sanjay, D. Stefan, S. Anna *et al.*, "Radiofrequency electromagnetic field exposure in everyday microenvironments in Europe: a systematic literature review", *J. Exp. Sci. Environ. Epidemiol.* **28** (2018), p. 147-160.
[14] Exem company, https://www.exem.fr/.
[15] P. Pinel, P. Tajan, Y. Poiré, L. Ourak, "EMF observatory, an answer to the societal debate", in *Proceeding of Journées scientifiques de l'URSI France*, 2020, p. 27-33.
[16] ANFR, "Protocole de mesure V4.1", https://www.anfr.fr/fileadmin/mediatheque/documents/expace/2017-08-28_Protocole_de_mesure_V4.pdf.
[17] EN IEC 62232, "Determination of RF field strength, power density and SAR in the vicinity of radiocommunication base stations for the purpose of evaluating human exposure", 2022, https://webstore.iec.ch/publication/64934.
[18] Annual report on In situ measurement web page on ANFR's website, https://www.anfr.fr/maitriser/les-installations-radioelectriques/etudes-sur-les-installations-radioelectriques/rapports-annuels-des-mesures.
[19] ANFR, "Study of the 5G contribution to exposure of the general public to electromagnetic waves", 2021, https://www.anfr.fr/fileadmin/mediatheque/documents/5G/20211214-exposition-5G-EN.pdf.
[20] "City hall square" report web page on ANFR's website, https://www.anfr.fr/maitriser/les-installations-radioelectriques/etudes-sur-les-installations-radioelectriques/mairies.
[21] I. T. Jolliffe, *Principal Component Analysis*, Springer, New York, NY, 2002.
[22] SEAWave Project, "5G and beyond", https://seawave-project.eu/.